tor would alter its hormone binding specificity and allow it to respond to human CG (hCG). This was not the case. As with the wild-type TSH receptor, these mutant TSH receptors were unresponsive to 10^{-7} M hCG, as measured by cAMP production (*11*).

The pituitary-placental glycoprotein hormone receptors represent a distinct subgroup in the G protein–coupled receptor family, whose members contain seven transmembrane spanning regions. The majority of the members of this receptor family, such as the α-adrenergic, β-adrenergic, muscarinic acetyl choline, and dopamine receptors (which we term group A), interact with small ligands and have insignificant extracellular regions. In contrast, the receptors for the very large glycoprotein hormones TSH, LH, CG, and follicle-stimulating hormone (FSH) (group B) have large extracellular domains (348 to 418 amino acids) (*3–5, 8, 12*). The largest extracellular domain is in the TSH receptor, primarily because of the presence of the 50–amino acid insertion. It is remarkable that this 50–amino acid tract that is unique to the TSH receptor was not important for TSH binding or signal transduction (cAMP generation). It is possible that this region serves a negative function, such as to prevent the binding of other ligands to the TSH receptor. However, deletion of the 50–amino acid segment did not allow the receptor to respond to hCG.

The data in this report provide strong evidence for the localization of a site for TSH binding to the eight–amino acid insertion of the TSH receptor. The amino acid sequence of the rat FSH receptor (*12*), reveals a unique ten–amino acid segment in the same general region (residues 21 to 30) as the eight–amino acid segment in the human TSH receptor. However, like the LH receptor, the FSH receptor does not contain the unique 50–amino acid segment of the TSH receptor (*3, 12*). The significance of this FSH receptor segment remains to be determined.

Identification of the epitopes on the TSH receptor that are recognized by auto-antibodies to the receptor in the sera of patients with Graves' disease is a subject of interest. These epitopes, which may or may not be identical to the TSH binding sites, may permit new diagnostic and therapeutic approaches to the management of patients with this common autoimmune disorder. The data in this report identify the eight–amino acid insert as an important site of action for both TSH and TSI.

REFERENCES AND NOTES

1. J. E. Dumont *et al.*, *Adv. Cyclic Nucleotide Res.* **14**, 479 (1981).
2. B. Rees Smith, S. M. McLachlan, J. Furmaniak, *Endocrinol. Rev.* **9**, 106 (1988).
3. Y. Nagayama, K. D. Kaufman, P. Seto, B. Rapoport, *Biochem. Biophys. Res. Commun.* **165**, 1184 (1989).
4. F. Libert *et al.*, *ibid.*, p. 1250.
5. M. Misrahi *et al.*, *ibid.* **166**, 394 (1990).
6. M. Parmentier *et al.*, *Science* **246**, 1620 (1989).
7. K. C. McFarland *et al.*, *ibid.* **245**, 494 (1989).
8. H. Loosfelt *et al.*, *ibid.*, p. **525**.
9. J. U. Bowie, J. F. Reidhaar-Olson, W. A. Lim, R. T. Sauer, *ibid.* **247**, 1306 (1990).
10. W. E. Hinds, N. Takai, B. Rapoport, S. Filetti, O. H. Clark, *J. Clin. Endocrinol. Metab.* **52**, 1204 (1981).
11. H. L. Wadsworth, G. D. Chazenbalk, Y. Nagayama, D. Russo, B. Rapoport, unpublished data.
12. R. Sprengel, T. Braun, K. Nikolics, D. L. Segaloff, P. H. Seeburg, *Mol. Endocrinol.* **4**, 525 (1990).
13. G. D. Chazenbalk, Y. Nagayama, K. D. Kaufman, B. Rapoport, *Endocrinology*, in press.
14. H. Hirayu, R. P. Magnusson, B. Rapoport, *Mol. Cell. Endocrinol.* **42**, 21 (1985).
15. Abbreviations for the amino acid residues are: A, Ala; C, Cys; D, Asp; E, Glu; F, Phe; G, Gly; H, His; I, Ile; K, Lys; L, Leu; M, Met; N, Asn; P, Pro; Q, Gln; R, Arg; S, Ser; T, Thr; V, Val; W, Trp; and Y, Tyr.
16. T. A. Kunkel, *Proc. Natl. Acad. Sci. U.S.A.* **82**, 488 (1985).
17. F. Sanger, S. Nicklen, A. R. Coulson, *ibid.* **74**, 5463 (1977).
18. C. Chen, and H. Okayama, *Mol. Cell. Biol.* **7**, 2745 (1987).
19. K. Kasagi *et al.*, *J. Clin. Endocrinol. Metab.* **62**, 855 (1986).

20. We recognize the contribution of F. Cohen and S. Presnell for their valued advice during the course of these studies and appreciate the expert administrative assistance of G. dela Calzada. Supported by NIH grants DK-36182 and DK-19289, and the Research Service of the Veterans' Administration.

20 June 1990; accepted 1 August 1990

Anatomy of a Conformational Change: Hinged "Lid" Motion of the Triosephosphate Isomerase Loop

DIANE JOSEPH, GREGORY A. PETSKO,* MARTIN KARPLUS

Triosephosphate isomerase (TIM) is used as a model system for the study of how a localized conformational change in a protein structure is produced and related to enzyme reactivity. An 11-residue loop region moves more than 7 angstroms and closes over the active site when substrate binds. The loop acts like a "lid" in that it moves rigidly and is attached by two hinges to the remainder of the protein. The nature of the motion appears to be built into the loop by conserved residues; the hinge regions, in contrast, are not conserved. Results of molecular dynamics calculations confirm the structural analysis and suggest a possible ligand-induced mechanism for loop closure.

CONFORMATIONAL CHANGES IN proteins are often an essential part of enzyme mechanisms (*1, 2*). Although x-ray crystallography provides structural data for highly populated species, such as the initial and the final states in a conformational change, other experiments and computer simulations are necessary to explore the motions involved. In this report, we combine molecular dynamics (MD) simulations with structural and sequence data to obtain a description of the so-called "loop transition" in the enzyme TIM. We show that the localized loop closure involves an essentially rigid-body type displacement, analogous to that implicated in the hinge bending domain motions of certain proteins (*3, 4*).

D. Joseph, Department of Chemistry, Massachusetts Institute of Technology, Cambridge, MA 02139, and Department of Chemistry, Harvard University, Cambridge, MA 02138.
G. A. Petsko, Department of Chemistry, Massachusetts Institute of Technology, Cambridge, MA 02139.
M. Karplus, Department of Chemistry, Harvard University, Cambridge, MA 02138.

*Present address: Rosenstiel Basic Medical Sciences Research Center, Brandeis University, Waltham, MA 02254–9110.

Yeast TIM is a dimer with two identical subunits, each composed of 247 residues. Although the monomers have identical noncooperative sites, only the dimer is catalytically competent. Each subunit contains a loop region (residues 166 to 176) (*5*) that projects into solvent in the unliganded enzyme and closes over the active site when substrate binds (Fig. 1) (*6*). Earlier low-resolution studies (*7*) and simulations (*8*) suggested that the loop was disordered in the open structure. The refined high-resolution structure of native TIM shows a single predominant conformation for the loop with high thermal parameters (*9*). In the refined high-resolution crystal structure of TIM complexed with the transition-state-intermediate analog phosphoglycolohydroxamate (PGH), the loop is closed and appears to be in the same position as in the enzyme-substrate complex (*10*). Mutagenesis experiments have shown that the loop is essential for catalysis (*11*).

When the open and closed structures of TIM are superimposed by least-squares optimization (*12*) of all α-carbons of subunit 1 (excluding residues 166 to 176), the root-

Fig. 1. A comparison of the closed and open structure of subunit 1; only α-carbons are shown. The two structures were superposed by least-squares optimization excluding the loop residues, which are shown in thick black lines.

mean-square (rms) deviation of the α-carbons is only 0.42 Å, whereas that for the loop residues is 4.8 Å. (We give the results for one subunit only, since those for the other subunit are similar.) Parts of the main chain of the loop move more than 7 Å in going from the open to the closed form. Specifically, the α-carbon of Thr^{172}, which is at the center of the loop (Fig. 2), is shifted by 7.1 Å, while the ends of the loop change little; for example, the distance from α-carbon 166 to α-carbon 176 is 7.3 Å in the open structure and 7.5 Å in the closed structure. There is a strikingly similar internal structure of the loop in the open and closed forms, in spite of the significant overall motion (Fig. 2); that is, when residues 166 to 176 in the initial and final states are superposed, the rms deviation for all loop atoms is only 0.73 Å.

These structural results suggest that a rigid-body, hinge-type motion takes place when the loop closes over the substrate in the active site. To identify the hinge regions, we plotted α-carbon pseudodihedral angle and main-chain dihedral angle differences between the open and closed loops versus residue number (*13*). From the α-carbon results (Fig. 3A), it is evident that there are two hinges. One of these involves the angles 166-167 and 167-168, and the other angles 174-175, 175-176, and 176-177 (we specify the pseudodihedral angle defined by the α-carbons $i - 1$, i, $i + 1$, $i + 2$ in terms of the central residue numbers i, $i + 1$). Changing only these angles from their values in the closed structure to their values in the open structure yields an "open loop" with an α-carbon rms difference of 1.9 Å from the open structure when nonloop α-carbons are superimposed. If the 164-165 pseudodihedral angle is also rotated from the closed to the open value, the α-carbon rms difference from the open structure is only 1.1 Å. This picture contrasts with that obtained from the dihedral angles ϕ and ψ (Fig. 3B). It is evident from the dihedral angle difference plots that motion occurs in the region of residues 174 and 175, but it is less evident that there is also a significant change in the region of residues 166 and 167. The largest loop dihedral angle differences are $\Delta\phi_{165} = 38°$, $\Delta\psi_{166} = -43°$, $\Delta\psi_{174} = 84°$, and $\Delta\phi_{175} = -63°$. These values are significantly greater than the average rms difference of 20° for nonloop main chain dihedral angles of subunit 1 relative to subunit 2 in both the open and closed forms. However, the large changes in ψ_{174} and ϕ_{175} are in the opposite direction and similar in magnitude (anticorrelated), so that the displacement of the backbone is somewhat reduced (*14*). If one uses $(\Delta\psi_{n-1} + \Delta\phi_n)$, which correlate well with the pseudodihedral angles (*15*), only 164-165, 166-167, 167-168, 174-175, 175-176, and 176-177 have values greater than 20°.

Comparison of the α-carbon pseudodihedral angle difference plots for the two nonequivalent subunits shows that they are similar (Fig. 3A). The main chain dihedral angle differences are also similar (Fig. 3B), except that the second subunit in the open structure has a large change in ψ_{171} and ϕ_{172} relative to the first subunit. Since $\Delta\psi_{171} = -55°$ and $\Delta\phi_{172} = 53°$, the anticorrelation is essentially exact and only a reorientation of the Gly^{171} to Thr^{172} peptide group results; the closed loop structures of the two subunits are nearly identical. The reorientation indicates there is some local flexibility in the open form of the loop. Examination of Ramachandran plots for the ϕ and ψ angles of the loop residues shows that they remain in the same allowed conformational region throughout the transition (right-handed α helix or β sheet, except for Gly^{171} and Gly^{173}, which are in the left-handed α-helix region). This result suggests that there are no large main chain energy barriers between the open and closed form.

To explain the location of the hinge regions, we examined the sequence conservation of the loop in the 13 different known TIM sequences (*16*). The loop is highly conserved compared to the rest of the protein. Overall, the enzymes from other species have sequence identity with yeast TIM ranging from 36 to 53%, and only 17% of the residues are strictly conserved in all TIMs. In contrast, loop residues 168 to 173 are strictly conserved, but residues 166, 167, and 174 to 176 are not. Because the central region of the loop is conserved rather than the hinges and the open and closed loop structures are very similar (Fig. 2), the loop

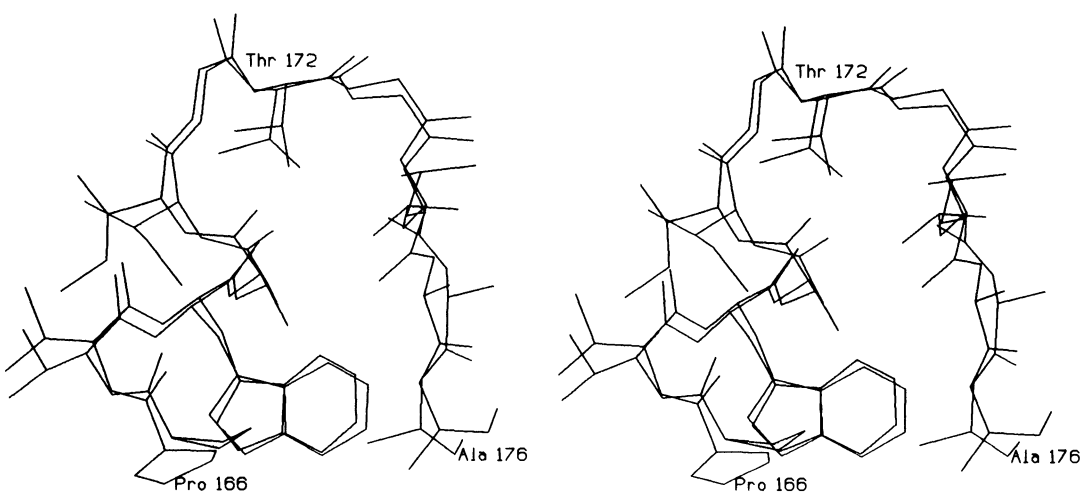

Fig. 2. A superposition of the closed and open structure loop residues, 166 to 176, by least-squares optimization of the loop atoms; all atoms are shown.

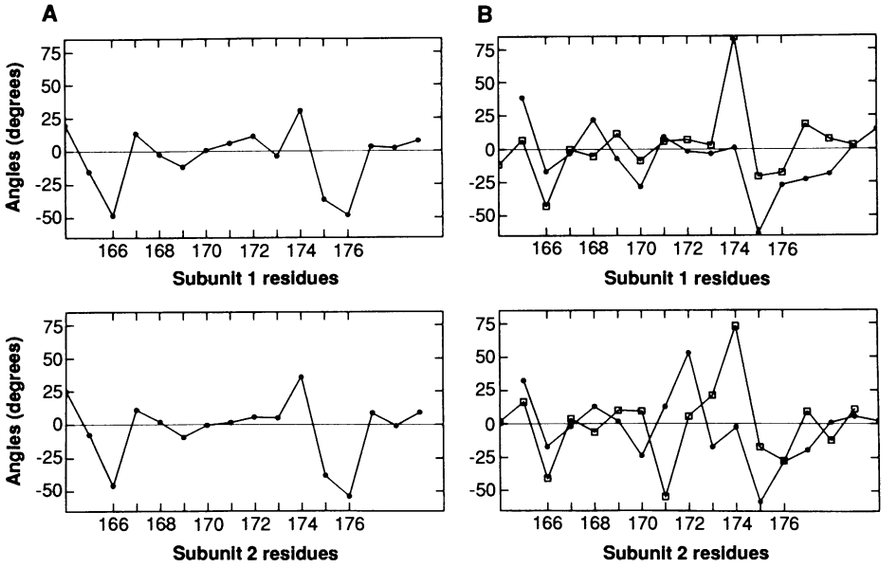

Fig. 3. Plots of closed minus open loop structure dihedral angle differences for subunit 1 and for subunit 2. (**A**) The α-carbon pseudodihedral angle differences and (**B**) main chain dihedral angle differences versus residue number. In (A) the number i corresponds to angle i, $i + 1$; in (B) circles represent relative ϕ and squares relative ψ.

acts more like a rigid lid with two hinges than a flexible loop. Van der Waals packing and hydrogen bonding within the loop contribute to the rigidity. Both the open and closed form of the loop are tightly packed except for a hole at the 174-175 hinge (Fig. 4). There is also a space above residues 165 and 166 in the closed form; when the loop opens, the side chain of Trp^{168} moves down and fills the space.

The loop residues are involved in a number of internal hydrogen bonds (*17*), in accord with the lid model (Fig. 5). The open structure has three intraloop hydrogen bonds and the closed structure has four. In the open structure, residues 171, 173, 175, and 176 make no hydrogen bonds to the rest of the protein, whereas in the closed structure only residue 175 makes no hydrogen bond (Fig. 5). The loop makes only one hydrogen bond to the substrate in the closed structure; that is, Gly^{171} donates a main chain NH hydrogen bond to a phosphate oxygen. In both structures, all of the hydrogen bonds between loop and nonloop residues are to side chain atoms of residues that are strictly conserved in the known 13 TIM sequences and that are not involved directly in substrate binding or catalysis. In the open structure Trp^{168} hydrogen bonds to Tyr^{164}, whereas in the closed structure Trp^{168} hydrogen bonds to Glu^{129}, Gly^{173} to Ser^{211}, and Ala^{176} to Tyr^{208}. The catalytic base, Glu^{165}, moves significantly toward the substrate in the closed structure; the position of the δ-carbon of Glu^{165} differs by 3.0 Å in the two structures. There is a concomitant displacement of the backbone atoms of Glu^{165}, Pro^{166}, Val^{167}, and Trp^{168}. The overall backbone atom rms deviation is 0.51 Å between the open and closed structure, whereas that for the backbone atoms of these four residues is 0.75 Å, 1.0 Å, 1.7 Å, and 2.9 Å, respectively. In the closed form a hydrogen bond between Trp^{168} and Tyr^{164} is broken and one between Trp^{168} and Glu^{129} is formed (*18*). This rearrangement may be a key to the pseudodihedral changes in the 166-168 region, which in turn allow the large changes in the 174-175 region that close the lid.

To obtain information about the lid motion, we performed several MD simulations. We used high temperatures to decrease the time required for a conformational change. All simulations began with the closed form, since an open structure with increased entropy was expected to be favored at high temperatures even in vacuum. To determine the appropriate temperature range, we performed simulations at 298, 500, and 1000 K of residues 167 to 178 alone, with the

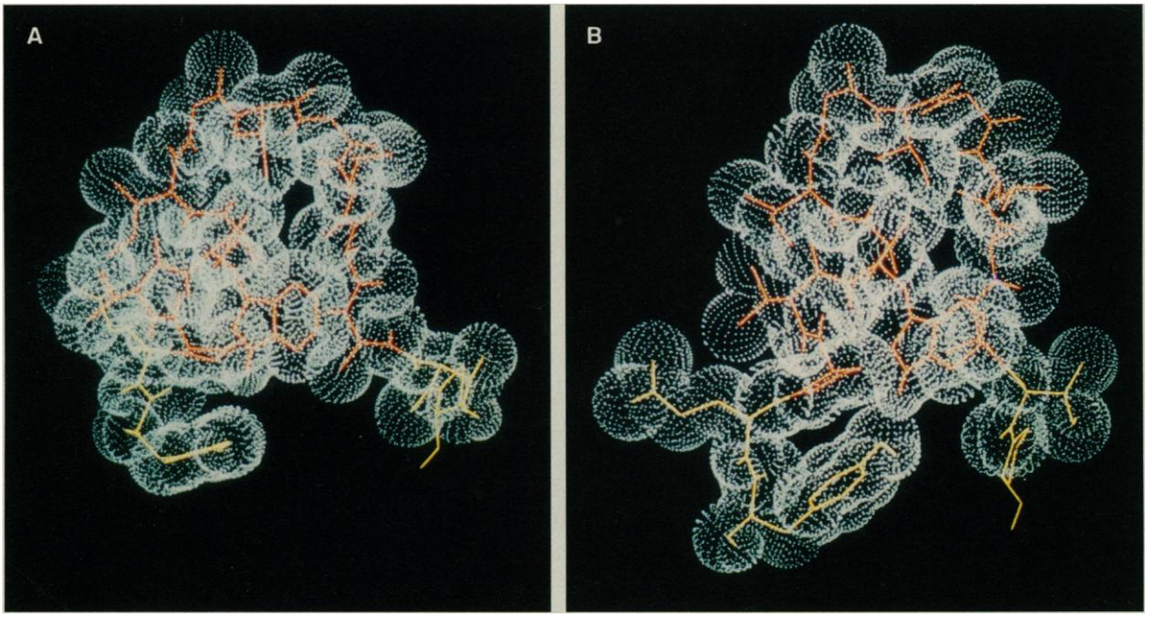

Fig. 4. Van der Waals dot surface representation for the (**A**) closed structure and (**B**) open structure; residues 164 to 178 are shown. Loop residues 166 to 176 are in red.

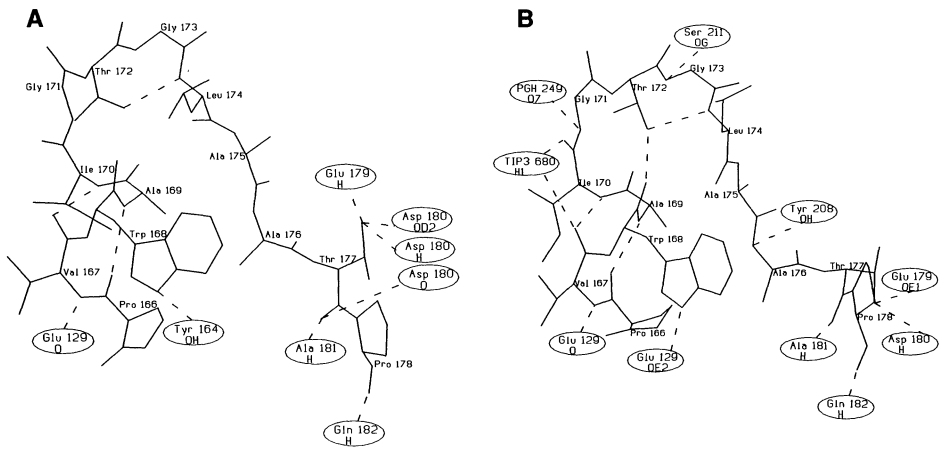

Fig. 5. The hydrogen bonding patterns of residues 166 to 178. (**A**) Open structure and (**B**) closed structure. Hydrogen bonds are represented as dash-dot lines.

main chain atoms of residues 167 and 178 fixed, and the side chain atoms of these residues deleted. At 298 K, the loop oscillated about the closed position, whereas during the 1000 K MD simulation the loop opened and closed repeatedly. During the 500 K MD simulation, the loop oscillated about the closed position until 29 ps, when it flipped to a more open position; the Thr^{172} α-carbon difference from the closed form was about 5.5 Å, somewhat less than the value of 7.1 Å found experimentally. Plots of the dihedral angle differences between the MD structure at 29 ps and the closed and open structures show the largest changes between residues 174 and 175. This suggests that the loop starts to open in the region of 174 and 175, in accord with the suggestion that the final step in closing involves these residues.

As a next approximation all of the atoms of subunit 1 were included in the simulation, but only residues 166 to 178 were allowed to move. Calculations were done for 30 ps with and without PGH at 1000 and 2000 K. At 1000 K the loop stayed closed even when PGH was removed. At 2000 K the loop stayed closed with PGH present and opened at 22 ps in the absence of PGH. This open loop conformation is, however, very different from that observed in the crystal structure. The Tyr^{164} OH to Trp^{168} HE1 hydrogen bond distance, which is 2.0 Å in the open form and 4.9 Å in the closed form, is 7.0 Å. The open loop conformation is twisted with the 174-175 end open and the other end closed in, suggesting that 2000 K is too high a temperature. To determine if the loop did not open at 1000 K without PGH because the strictly conserved nonloop residues that make important hydrogen bonds to the loop were fixed in the simulation, we repeated the 1000 K MD simulation, but allowed residues 129, 211, and 164 to 178 to move. (Tyr^{208} was not included in the mobile residues, since its position is so similar in the open and closed structures.) At 19 ps the loop starts to open, and then continues to oscillate about this open position for the rest of the 60 ps simulation. The Thr^{172} α-carbon moved about 5 Å in the open direction. Many times throughout the simulation the Tyr^{164} OH to Trp^{168} HE1 distance was 3.5 Å, midway between the closed and the open values determined experimentally. At 28 ps, one of the coordinate sets that most resembled the open structure, the largest jumps in the dihedral differences are between 169, 170, and 171, with ψ_{174} and ϕ_{175} midway between the experimental closed and open values. Also at 28 ps, the hydrogen bonds that the loop in the closed form makes to nonloop residues Glu^{129}, Ser^{211}, and Tyr^{208} have all broken, but the hydrogen bond to Tyr^{164} of the open form has not yet formed. It is not surprising that the loop never completely opens, because the simulations are in vacuum and stabilization of the open structure by solvent is not included.

The present analysis shows that the TIM loop behaves more like a lid than a flexible loop and suggests that similar behavior may be found in other enzymes that are known to contain loop regions that protect the active site after substrate is bound. The lid motion is localized primarily at the pseudo-dihedral angle hinges 166-167, 167-168 and 174-175, 175-176. The displacement of Glu^{165} on substrate binding may initiate the loop closure; that is, such a positional change may move the neighboring backbone atoms sufficiently to weaken the Trp^{168}-Tyr^{164} hydrogen bond, so as to release the indole of Trp^{168} to interact with Glu^{129}. A cascade of dihedral angle changes would then occur culminating in those involving 174-175 that close the loop. Tests of this mechanism can be made experimentally by mutagenesis and theoretically by simulations that include solvent (*19–21*) and determine the reaction path or paths (*22*) in going from the closed form to the open form and vice versa.

REFERENCES AND NOTES

1. W. S. Bennett and R. Huber, *CRC Crit. Rev. Biochem.* **15**, 291 (1984).
2. C. L. Brooks III, M. Karplus, B. M. Pettitt, *Adv. Chem. Phys.* **71**, 1 (1988).
3. J. A. McCammon, B. R. Gelin, M. Karplus, P. G. Wolynes, *Nature* **262**, 325 (1976).
4. J. Janin and S. Wodak, *Prog. Biophys. Mol. Biol.* **42**, 21 (1983).
5. The exact boundary of the loop depends on the definition used. We use the location of the hinges described in this paper to set the residue limits.
6. T. Alber *et al.*, *Cold Spring Harbor Symp. Quant. Biol.* **52**, 603 (1987).
7. T. Alber *et al.*, *Philos. Trans. R. Soc. London B* **293**, 159 (1981).
8. F. K. Brown and P. A. Kollman, *J. Mol. Biol.* **198**, 533 (1987).
9. E. Lolis *et al.*, *Biochemistry* **29**, 6609 (1990). We added hydrogens with the program CHARMM (version 20) [B. R. Brooks *et al.*, *J. Comp. Chem.* **4**, 187 (1983)] and the routine Hbuild [A. T. Brünger and M. Karplus *Proteins* **4**, 148 (1988)] and then subjected the structure to 200 steps of Powell minimization with decreasing harmonic constraints.
10. R. C. Davenport, Jr., B. A. Seaton, P. A. Bash, G. A. Petsko, in preparation.
11. D. L. Pompliano, A. Peyman, J. R. Knowles, *Biochemistry* **29**, 3186 (1990).
12. The program HYDRA on an Evans and Sutherland PS300 molecular graphics system was used (copyright Polygen Corporation 1986, 1987).
13. All dihedral angle, energy minimization, and MD calculations were performed with the CHARMM program (version 20). The MD calculations consisted of 5 ps of heating with the initial temperature 100 K and velocities assigned from a Gaussian distribution. This was followed by 5 ps of equilibration. The equations of motion were integrated with the Verlet algorithm with a step size of 1 fs. Distances of bonds to hydrogens were constrained with SHAKE, a distance-dependent dielectric was used, and a switching function to truncate the long-range nonbonded interactions at 9.0 Å. The standard polar hydrogen potential function parameters (PARAM 19) of CHARMM 20 were used.
14. J. A. McCammon, B. R. Gelin, M. Karplus, *Nature* **267**, 585 (1977).
15. W. L. Peticolas and B. Kurtz, *Biopolymers* **19**, 1153 (1980).
16. TIM sequences from 12 different organisms have been aligned by E. Nickbarg [thesis, Harvard University, Cambridge, MA (1988)]; an additional sequence was obtained from S. E. Old and H. W. Mohrenweiser, *Nucleic Acids Res.* **16**, 9055 (1988).
17. The HYDRA hydrogen bond search routine was used with the default parameters [E. N. Baker and R. E. Hubbard, *Prog. Biophys. Mol. Biol.* **44**, 97 (1984)].
18. When the open and closed structures are superimposed, the δ-carbons of Glu^{129} are 1.43 Å apart. This difference appears to be due to the hydrogen bond between the carboxylate of Glu^{129} and the indole NH of Trp^{168} that is only present in the closed form. In the open form, the Trp^{168} NH is hydrogen-bonded to the phenolic OH of Tyr^{164}.
19. C. L. Brooks III and M. Karplus, *J. Chem. Phys.* **79**, 6312 (1983).
20. A. T. Brünger, C. L. Brooks III, M. Karplus, *Chem. Phys. Lett.* **105**, 495 (1984).
21. C. L. Brooks III, A. T. Brünger, M. Karplus, *Biopolymers* **24**, 843 (1985).
22. R. Elber and M. Karplus, *Chem. Phys. Lett.* **139**, 375 (1987).

23. We thank S. Almo, R. C. Davenport, E. Lolis, D. Nguyen, and N. Summers for their insightful conversation. Supported in part by grants from the NSF, NIH, and the Department of Energy.

27 March 1990; accepted 22 June 1990